Static and dynamical properties of circular NiFe/Cu/Co nanodisks

P. Vavassori, V. Bonanni, A. Busato, G. Gubbiotti, M. Madami et al.

Additional information on J. Appl. Phys.

Static and dynamical properties of circular NiFe/Cu/Co nanodisks

P. Vavassori,[a)] V. Bonanni, and A. Busato
CNISM, CNR-INFM S3, CIC nanoGUNE Consolider and Dipartimento di Fisica, Università di Ferrara, via Saragat 1, 44100 Ferrara, Italy

G. Gubbiotti and M. Madami
CNISM, Dipartimento di Fisica, Università di Perugia, Via A. Pascoli, I-06123 Perugia, Italy

A. O. Adeyeye, S. Goolaup, and N. Singh
Department of Electrical and Computer Engineering, National University of Singapore, 117575 Singapore

C. Spezzani
Sincrotrone Trieste S.C.p.A., I-34012 Trieste, Italy

M. Sacchi
Synchrotron SOLEIL, L'Orme des Merisiers, BP48, 91192 Gif-sur-Yvette, France

We present an experimental investigation of the static and dynamical properties of array of $Ni_{80}Fe_{20}$ (10 nm)/Cu (10 nm)/Co (10 nm) disks with diameter of 230 nm and edge-to-edge spacing of 160 nm. Magnetization reversal process studied by superconducting quantum interference device magnetometry, resonant scattering of polarized soft x-ray, and three-dimensional micromagnetic simulations reveals that the interlayer magnetostatic interaction and the different coercivities of the two layers are the key factors that determine the magnetization reversal of the disks through a sequence of antiparallel states. The dynamical properties were studied by Brillouin light scattering and micromagnetic simulations which solve the discretized Landau-Lifshitz-Gilbert equation in the time domain and calculated locally the Fourier transform. The comparison between measurements and simulations allowed us to correlate the field dependence of different modes in each ferromagnetic layer to their localization inside the disk. © *2008 American Institute of Physics*. [DOI: 10.1063/1.2835092]

The magnetization dynamics of laterally confined elements composed of alternating magnetic and nonmagnetic layers is an interesting and challenging research field. The effect of the interlayer dipolar coupling is the formation of either "acoustic" (in-phase) or "optic" (in antiphase) coupled spin wave modes[1–6] and, in addition, this can lead to modifications and distortions of the mode spatial distribution. Patterned multilayer stacks, have been proposed as basic units in the magnetic random access memory technology and are of current interest also in spintronics since, when an ac current is injected into the structure, spin waves can be excited through the so-called spin-transfer torque effect.[7] The reversal of such elements might be particularly complex because of the interplay between the interlayer magnetostatic interaction, brought about by the lateral confinement, and the asymmetry of the ferromagnetic layers typically employed in such structures (either different thickness and/or different materials).

Along these lines, in this paper, we have investigated the static and dynamical properties of nanoscale size multilayered disks consisting of Permalloy [$Ni_{80}Fe_{20}$ (NiFe)] and Co ferromagnetic layers separated by a 10 nm thick Cu spacer layer. Large area (4×4 mm^2) squared array of disk shaped NiFe (10 nm)/Cu (10 nm)/Co (10 nm) pseudospin valve nanostructures were fabricated using deep ultraviolet lithog-

raphy at 248 nm exposing wavelength on Si(001). The disks have diameter d=230 nm and edge-to-edge spacing s =160 nm (see inset of Fig. 1). A continuous NiFe/Cu/Co trilayer was also prepared and used as reference sample. For the magnetic characterization, we employed superconducting quantum interference device (SQUID) magnetometry and resonant scattering of polarized soft x-ray (XRMS) performed at the Circular Polarization beamline (CIPO) at ELETTRA synchrotron.[8] Hysteresis loops were measured in the longitudinal configuration with magnetic field applied in the sample plane and parallel to the[10] direction of the disks array. While SQUID probes the total magnetic moment of the patterned structure, XRMS is an element sensitivity technique which enabled us to obtain the magnetization curve of the NiFe and Co layers, separately. This was achieved by tuning the photon energy to the L_3 Fe and Co edges at 707 and 777 eV, respectively. Spin wave modes properties were studied by Brillouin light scattering (BLS) technique. A reversible magnetic field H was applied parallel to the array plane and perpendicular to the incident light beam, which has an incidence angle of 10° with respect to the sample normal.

The measured hysteresis loop and the spin wave frequencies and profiles were simulated by three-dimensional micromagnetic simulations performed by using the OOMMF package.[9] The disks were discretized into cells of $5 \times 5 \times 10$ nm^3 and the magnetic parameters used for polycrystalline Permalloy and cobalt are the following: M_s (NiFe)

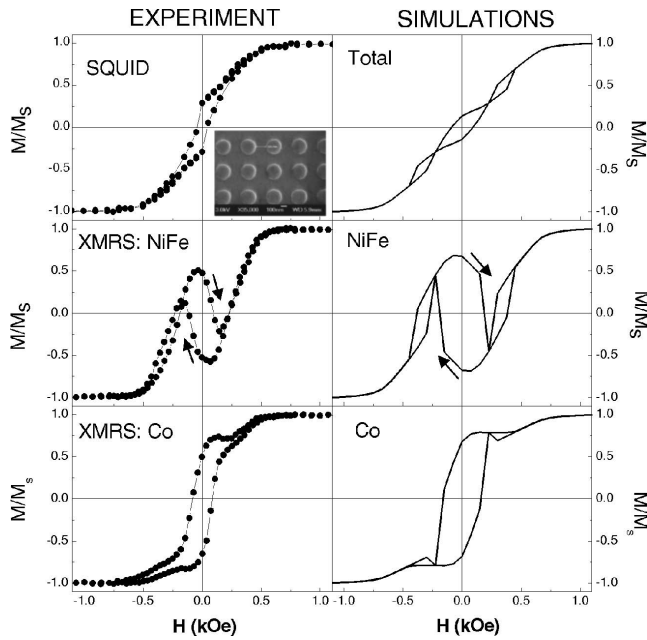a)Electronic mail: p.vavassori@nanogune.eu.

FIG. 1. (Left column) Normalized magnetic hysteresis curves measured by SQUID and XMRS. (Right column) Simulated hysteresis loop for the whole structure (first row) and for the NiFe and Co layer.

$=800\times10^3$ A/m and M_s (Co)$=1200\times10^3$ A/m for the saturation magnetization and A (NiFe)$=10\times10^{-13}$ J/m and A (Co)$=21\times10^{-13}$ J/m for the exchange stiffness constant. These magnetic parameters were derived from the BLS investigation of the continuous NiFe/Cu/Co reference trilayer. Magnetocrystalline anisotropy was neglected and the disks were considered as noninteracting. The OOMMF code has been modified so to provide as output both the total magnetic moment of the layered disk as well as the magnetic moment of the two NiFe and Co layers separately. Calculations of the modes frequencies and spatial were performed by solving the discretized Landau-Lifshitz-Gilbert equation over the layered structure in the time domain and performing a local Fourier transform.[10] The two-dimensional spatial distribution of each eigenmode corresponding to a particular frequency peak is obtained both for the NiFe and Co disks by plotting the imaginary part of the Fourier coefficient for each cell at the eigenmode frequency. In reporting these mode spatial distribution, we plot the component of the magnetization vector perpendicular to the sample plane (m_z) which gives the main contribution to the BLS cross section.[11]

In the left-hand panels of Fig. 1, the measured SQUID and XMRS loops are shown. SQUID magnetometry probes the total magnetization behaviour, while XRMS provides with the magnetization curve of the NiFe and Co layers separately. For this reason, the XMRS loops reveal more details

of the magnetization reversal process. Particularly interesting is the oscillating behavior of the magnetization in the NiFe layer evidenced by the corresponding XRMS loop.

The micromagnetic simulations reproduce quite well the measured SQUID and XMRS loops (see right panel of Fig. 1). The corresponding calculated micromagnetic configurations shown in Fig. 2 enable us to understand the magnetization curves measured by XMRS for the NiFe and Co layers. As the external field is reduced from positive saturation to zero, the magnetization of the central portion of the NiFe layer rotates first by 135° *clockwise* in a continuous way from being parallel to the applied field (see the corresponding sequence of magnetization configurations at 750, 500, 250, and 0 Oe shown in Fig. 2) determining the smooth drop to negative values of the XRMS signal (magnetization projection along the field direction) observed in the NiFe loop as the field is reduced to zero. In the same field range, the magnetization of Co rotates by 45° *counterclockwise* yielding to a smaller reduction of the XRMS in the Co loop. Therefore, in the remanent state, the magnetization of the two layers reaches a perfect antiparallel alignment (compare the two magnetization configurations at 0 Oe in Fig. 2), with its direction at almost 45° with respect to the direction of the external applied field. This configuration at remanence is clearly due to the dipolar interaction between the layers, which forces their magnetization to be antiparallel when no external field is applied.

As the field is further reduced to negative values, at a critical field intensity, the magnetization of the Co layer suddenly rotates by 90° counterclockwise causing a corresponding rotation by 45°, in the same direction, of the magnetization of the dipolar-coupled NiFe-layer (see the magnetization configurations at −250 Oe in Fig. 2). These rotations produce an increase of the XRMS signal in the NiFe loop (it comes back to positive values) and a decrease of the signal in the Co loop. At higher negative field values, the magnetization of the NiFe layer rotates once more by 45°, but this time clockwise, driven by the external field, while the magnetization of Co remains substantially fixed (see magnetic configurations at −500 Oe in Fig. 2). Finally, as the external field is increased further toward negative saturation values, the magnetization in both layers aligns gradually along the field direction. It is worth noting here that micromagnetic simulations explain the dominance of the magnetostatic dipolar interaction as due to the fact that the magnetization of both layers remains in a nearly single domain state during the entire reversal process. It is worth mentioning here that magnetization reversal dominated by the interlayer magnetostatic interaction in similar NiFe/Cu/NiFe patterns has been reported in the literature.[1,12] What makes the reversal of the
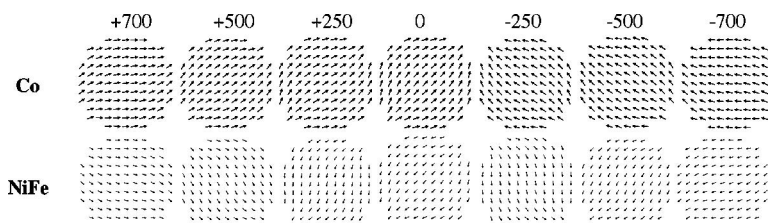

FIG. 2. Simulated magnetization distributions in the two layers (upper panel Co and lower panel NiFe) for different values of the applied field H.
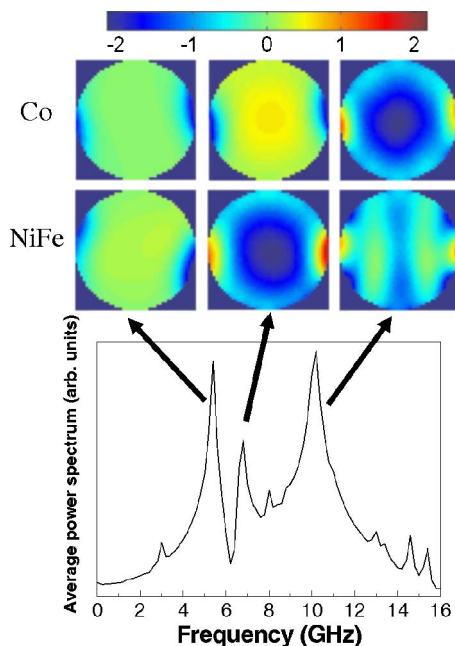
FIG. 3. (Color online) Calculated average power spectrum of the NiFe/Cu/Co disks for $H = 1.0$ kOe applied horizontally.
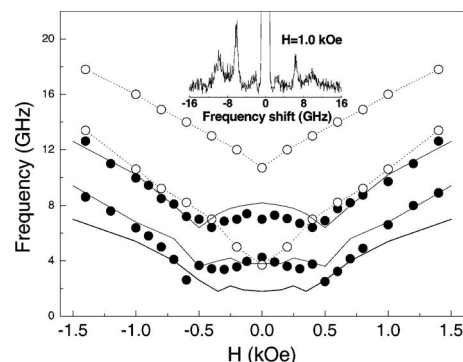

FIG. 4. Measured frequencies vs H from positive to negative saturation for the NiFe/Cu/Co disks (full points) and the continuous NiFe/Cu/Co trilayer (open points). Continuous and dotted curves are results of calculations.

NiFe/Cu/Co dots studied here more interesting and rich in term of intermediate states are the additional effects of the different coercive fields and saturation magnetizations in the two layers.[13]

In Fig. 3, we report the calculated averaged power spectrum, obtained for a bias field value of 1.0 kOe. We found that three principal peaks are active in the scattering process. Considering that the layers magnetization remains always in a single domain state, the magnetic eigenmodes classification is similar to that described in Ref. 14. The mode at 5.4 GHz is an end mode with the magnetization of the two layers oscillating in-phase near the particle edges. For this mode, the magnetization in the two layers oscillates in phase. The mode at 6.8 GHz has the character of the fundamental (F) mode of the NiFe layer, hybridized with and end mode, presenting only a weak magnetization oscillation in the Co layer. Similarly, the mode at 10.2 GHz corresponds to the fundamental mode of the Co layer and to a backwardlike mode in the NiFe layer, even if with a reduced oscillation amplitude. Both these modes are hybridized with an end mode. These results are different from what we have previously found for NiFe/Cu/NiFe disks[1] where the spatial mode distribution in the two layers has always the same symmetry and amplitude. A closer inspection of the spatial profiles for the modes at 6.8 and 10.2 GHz reveals an in-phase and out-of-phase precessional motions of the dynamical magnetizations in the two layers, respectively. The field evolution of the above mentioned modes have been compared to the measured values and the results are shown in Fig. 4. Here, the sample has been saturated in a positive field of 1.5 kOe which was then reduced to zero and reversed. Two broad peaks are present in the BLS spectra for the NiFe/Cu/Co disks as shown in the inset of Fig. 4 whose

frequency values are always smaller than those measured for the continuous (unpatterned NiFe/Cu/Co trilayer) used as reference sample (open points in Fig. 4). On reducing the field intensity, the frequency of all the modes decreases monotonously and reaches a minimum at about 0.5 kOe, which corresponds to the saturation field measured by SQUID (see Fig. 1). On further decreasing the field intensity, the frequencies of the modes start to increase again, reflecting the rotation of the magnetizations of the two layers. On the contrary, for the continuous NiFe/Cu/Co trilayer, we have found a monotonic decrease of the frequencies when the field is reduced to zero. It is noteworthy that the field dependence of the lowest frequency mode is well reproduced in the region between 0.35 and 0.7 kOe by both the fundamental NiFe mode and the end mode because of occurrence of hybridization effects.

[1]G. Gubbiotti, M. Madami, S. Tacchi, G. Carlotti, and T. Okuno, Phys. Rev. B **73**, 144430 (2006).
[2]K. W. Chou, A. Puzic, H. Stoll, G. Schütz, B. Waeyenberge, T. Tyliszczak, K. Rott, G. Reiss, H. Brückl, I. Neudecker, D. Weiss, and C. H. Back, J. Appl. Phys. **99**, 08F305 (2006).
[3]D. V. Berkov and N. L. Gorn, "Magnetodipolar interlayer interaction effect on the magnetization dynamics of a trilayer square element with the Landau domain structure," submitted to , full-text available from http://arxiv.org/abs/0707.2344..
[4]G. Gubbiotti, M. Kostylev, N. Sergeeva, M. Conti, G. Carlotti, T. Ono, and A. Stashkevich, Phys. Rev. B **70**, 224422 (2004).
[5]G. Gubbiotti, G. Carlotti, T. Ono, and Y. Roussigné, J. Appl. Phys. **100**, 023906 (2006).
[6]N. A. Sergeeva, M. Chérif, A. Stashkevich, M. P. Kostylev, and J. Ben Youssef, J. Magn. Magn. Mater. **288**, 250 (2005).
[7]S. I. Kiselev, J. C. Sankey, I. N. Krivorotov, N. C. Emley, M. Rinkoski, C. Perez, R. A. Buhrman, and D. C. Ralph, Phys. Rev. Lett. **93**, 036601 (2004).
[8]www.elettra.trieste.it/experiments/beamlines/polar/index.html for more details about the beamline.
[9]M. J. Donahue and D. G. Porter, OOMF User's Guide, Version 1.2 alpha 4 (NIST, Gaithersburg, MD, 2004).
[10]R. D. McMichael and M. D. Stiles, J. Appl. Phys. **97**, 10J901 (2005).
[11]G. Gubbiotti, G. Carlotti, T. Okuno, M. Grimsditch, L. Giovannini, F. Montoncello, and F. Nizzoli, Phys. Rev. B **72**, 184419 (2005).
[12]K. S. Buchanan, K. Yu. Guslienko, A. Doran, A. Scholl, S. D. Bader, and V. Novosad, Phys. Rev. B **72**, 134415 (2005).
[13]J. X. Zhang and L. Q. Chen, J. Appl. Phys. **97**, 084313 (2005).
[14]L. Giovannini, F. Montoncello, F. Nizzoli, G. Gubbiotti, G. Carlotti, T. Okuno, T. Shinjo, and M. Grimsditch, Phys. Rev. B **70**, 172404 (2004).